Microwave Engineering
Ulm University

ulm university universität
uulm

# Towards a mm-Wave Planar Biomimetic Antenna Array with Enhanced Phase Sensitivity

Patrik Grüner, Tobias Chaloun, and Christian Waldschmidt


DOI: 10.1109/EuCAP.2016.7481535

# Towards a mm-Wave Planar Biomimetic Antenna Array with Enhanced Phase Sensitivity

Patrik Grüner, Tobias Chaloun, and Christian Waldschmidt
Institute of Microwave Engineering, University of Ulm, Ulm, Germany, patrik.gruener@uni-ulm.de

***Abstract*—The design and measurements of a two-element biomimetic antenna array is presented with enhanced phase sensitivity at 20 GHz using planar structures only. The antenna array hereby mimics the hearing system of the parasitoid fly *Ormia ochracea*. To the authors' knowledge, this is the first biomimetic antenna array using frequencies above 1 GHz. Using an aperture coupled patch antenna array with element spacing of $\lambda/5$ and a corresponding external coupling network a phase gain of 5 has been achieved. The proposed architecture is supposed to be usable in even higher frequency bands, especially in the mm-wave range.**

***Index Terms*—Biomimetic antennas, Enhanced phase sensitivity, Planar antennas.**

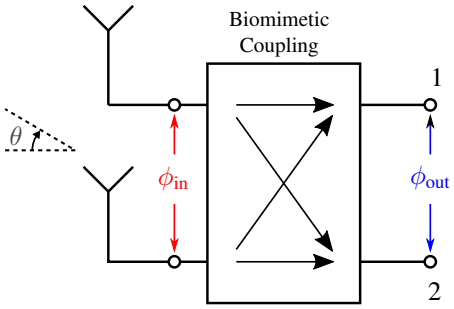


Fig. 1. Principle of the biomimetic antenna array (BMAA).

## I. Introduction

Angle estimation with antenna arrays is usually done by evaluating the phase progression from one antenna element to the other. This phase progression is directly dependant on the element separation and so it is desirable to put the antenna elements as far apart as possible without getting ambiguity. However, if the available space is limited and the wavelength is large compared to the antenna array, the angle estimation of the incoming plane wave becomes more and more difficult.

Looking in the nature, the parasitic fly *Ormia ochracea* is facing a similar challenge. This fly is dependant on a live field cricket on which it deposits its larvae and which serves as food for the larvae. To localize this cricket, the fly relies on the meeting call of the cricket which has a frequency of around 5 kHz [1]. Comparing the wave length of the sound wave at 5 kHz (ca. 70 mm) and the separation of the ears of *Ormia ochracea* (about 1.5 mm), there should not be any angle estimation possible according to classical theory. However, *Ormia ochracea* is able to localize the cricket with an accuracy of about 2°. This is done by a hearing system consisting of two strongly coupled ears, which acts as a phase amplification system.

Numerous research projects have been reported previously to adapt the principle of this hearing system to technical systems [2]–[5]. In [6] a thorough examination of the biomimetic antenna array (BMAA) was presented. The results show the feasibility to design this antenna system in the 600 MHz range with given parameters. Also a fundamental tradeoff between phase sensitivity and output power level was presented. This seems to be characteristic for this antenna system.

The key parts of the system are a two element array with strong mutual coupling and an external coupling network, see Fig. 1. The input phase difference is defined as $\phi_{\text{in}} = kd\sin(\theta)$ and depends on the physical separation $d$ of the antenna elements. The output phase difference, however, is defined as $\phi_{\text{out}} = \arg(u_1) - \arg(u_2)$, with $u_1$ and $u_2$ the complex voltages at the antenna terminals.

In the present work, a first Biomimetic Antenna Array (BMAA) for the upper microwave range is designed and evaluated by transferring and expanding the current system models to the 20 GHz range. All components are realized in planar PCB technology which enables very easy and cost efficient fabrication.

## II. System Model

The system model used for designing the BMAA is based on the work presented in [2] and uses basically the same design process for the dimensioning of the coupling network. However, some adaptions are needed for the use in the 20 GHz range.

The electrical system model was derived from the mechanical model of the hearing system of *Ormia ochracea* [1]. It models the respective antenna elements as current sources characterized by their Y-Parameters (Fig. 2). Due to

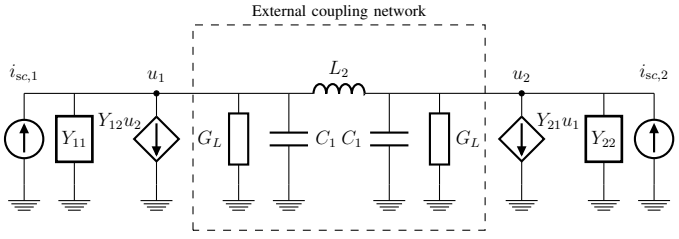


Fig. 2. Equivalent circuit model derived from mechanical model of the hearing systems of *Ormia ochracea* [2].

the close proximity of the radiating elements, the current sources are modeled with equal excitation amplitudes and slightly different phases depending on the angle of incidence $\theta$. The mutual coupling of the antenna elements is modeled by voltage controlled current sources, also characterized by their Y-Parameters. In this design, the biomimetic coupling consists of an inductor $L_2$ and two capacitors $C_1$ to couple the two antenna elements externally. The advantage of this structure compared to the network used e.g. in [6] is that no lossy transformers have to be used. This enables the use in higher frequency bands.

A typical phase difference $\phi_{\text{out}}$ at the output of the system is shown in Fig. 3. The phase difference $\phi_{\text{in}}$ at the input of the

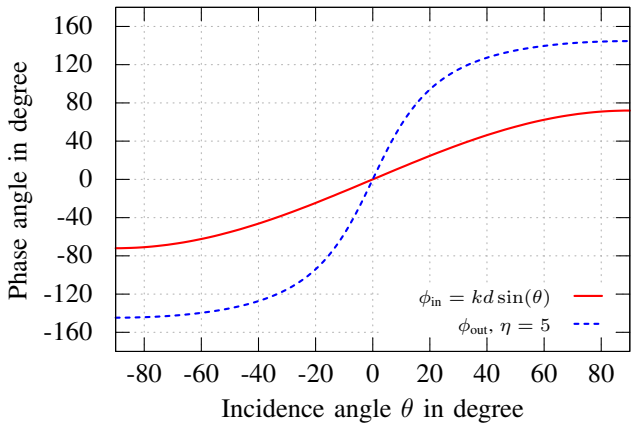


Fig. 3. Simulated phase difference at the output of a conventional array (solid red) and a biomimetic antenna array (dashed blue) with a phase gain of $\eta = 5$.

antennas is set by the physical separation of the respective antenna elements and therefore depends on the angle of incidence $\theta$ and the element separation $d$. At the output of the antenna array, the phase difference $\phi_{\text{out}}$ is expanded compared to $\phi_{\text{in}}$.

As a measure to characterize the BMAA, the terms phase gain $\eta$ and normalized output power $P^n_{\text{out}}$ were proposed in [2]. The definition of the phase gain is given by the quotient of the slopes of the respective phase differences of an uncoupled antenna array ($\phi_{\text{in}}$) and after the biomimetic coupling ($\phi_{\text{out}}$) in boresight direction:

$$\eta = \frac{\left.\frac{\mathrm{d}\phi_{\text{out}}}{\mathrm{d}\theta}\right|_{\theta=0}}{\left.\frac{\mathrm{d}\phi_{\text{in}}}{\mathrm{d}\theta}\right|_{\theta=0}} . \tag{1}$$

In Fig. 3 a phase gain of $\eta = 5$ is set, resulting in a $\phi_{\text{out}}$ slope five times steeper than the $\phi_{\text{in}}$ slope at boresight.

For the reduction of the output power level a new dimensionless quantity $L_{\text{out}}$ is defined (which is similar to $P^n_{\text{out}}$ in [2]):

$$L_{\text{out}} = \frac{P_{\text{out,BMAA}}}{P_{\text{out,reg. Array}}} . \tag{2}$$

This quantity indicates the power level at the output of the BMAA compared to a regular array using the same radiating elements with similar separation but no external coupling network.

## III. Antenna Design

The BMAA design process is divided into two parts. First, an antenna array with strong mutual coupling is designed. With the Y-parameters from this antenna array the coupling network for the BMAA can be designed for a specific parameter set ($\eta$, $L_{\text{out}}$) in a second step.

### A. Antenna Array with Strong Mutual Coupling

In the present work a rectangular patch antenna is chosen as radiating element. To allow for a strong mutual coupling as well as a small aperture, the radiating elements are placed in the H-Plane next to each other. The coupling network is supposed to be placed on the same substrate in the next design step. To avoid disturbance of the radiation pattern due to possible parasitic radiation of the feeding and coupling network, a two-layer process was chosen. The patch antennas are located on one side of a 508 µm thick RO3003 substrate from Rogers Corporation with permittivity $\varepsilon_r = 3$ and are fed through an H-shaped aperture. The microstrip lines feeding the antenna are located on a second RO3003 substrate with a thickness of 127 µm. Both substrates are laminated using a RO3001 bonding film. The model of the antenna array with strong mutual coupling is shown in Fig 4.

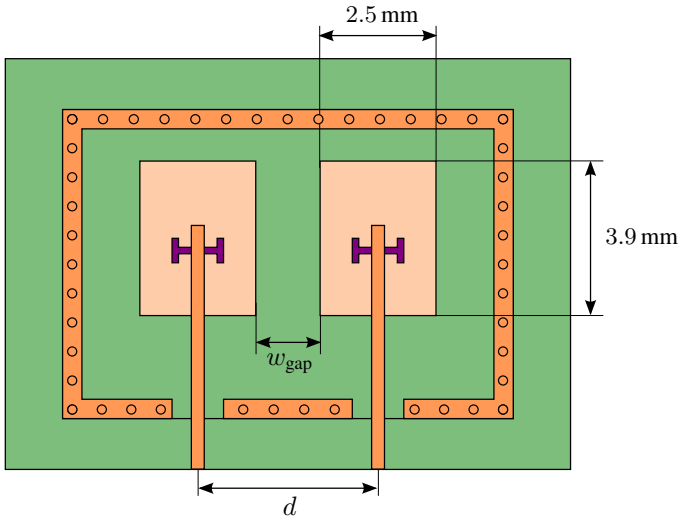


Fig. 4. Bottom view at the layout of the proposed antenna array with strong mutual coupling. The patches and the H-shaped coupling apertures are shown for orientation (drawing without scaling).

The distance $w_{\text{gap}}$ between the elements is the key parameter to control the strength of the mutual coupling. Figure 5 shows the effect of the variation of $w_{\text{gap}}$ on the mutual coupling. As expected the mutual coupling increases as the elements get closer together. Figure 6 shows the achievable maximum phase gain $\eta_{\text{max}}$ for the same separations of the antenna elements. It can be clearly seen that the maximum phase gain $\eta_{\text{max}}$ in boresight direction depends significantly on a strong mutual coupling. While for a standard array with a half-wavelength

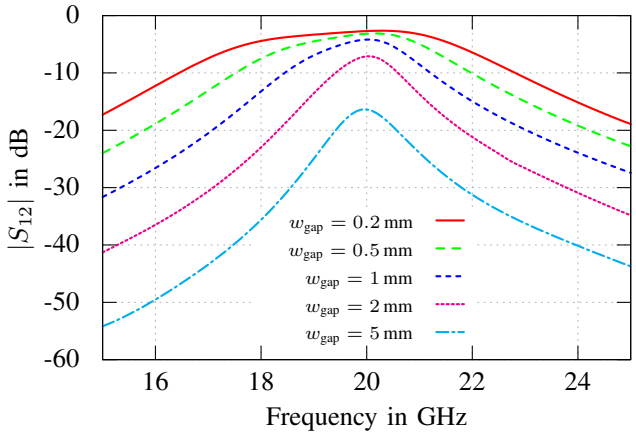


Fig. 5. Simulated $|S_{12}|$ for different distances $w_{gap}$ between the antenna elements. $w_{gap} = 5\,\text{mm}$ corresponds to an element distance of $d = \lambda/2$.

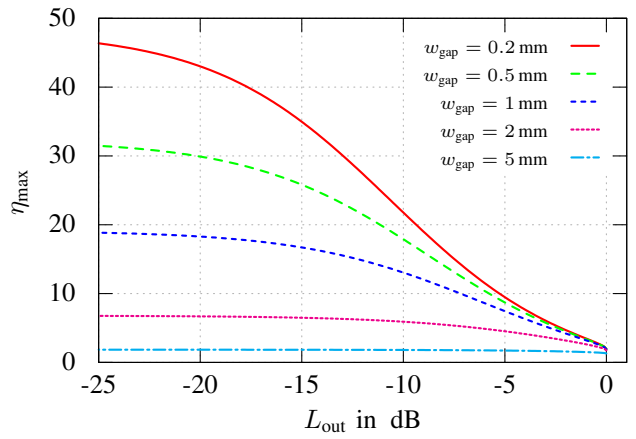


Fig. 6. Simulated maximum phase gain $\eta_{max}$ as a function of the output level $L_{out}$ and the antenna element separation $w_{gap}$ for the proposed antenna.

separation between the antenna elements ($w_{gap} = 5\,\text{mm}$) almost no phase gain can be achieved, the phase gain keeps increasing for smaller distances and therefore higher mutual coupling.

From the investigated parameters $w_{gap} = 0.5\,\text{mm}$ was chosen, giving a mutual coupling of about $-3\,\text{dB}$ and a maximum phase gain of well above 10 for an output level less than $-6\,\text{dB}$.

### B. Proposed Coupling Network Scheme

Using the system model from Section II and the Y-Parameters of the planar antenna array, the unknown element values $C_1$, $L_2$, and $G_L$ were calculated to achieve a phase gain of $\eta = 8$ with an output level of $L_{out} = -5\,\text{dB}$. The calculated values are given in Tab. I. Due to the very small element values a realization by means of lumped elements is supposed to be impossible because the package inductances and capacitances of SMDs may be higher than the nominal value. Therefore, a new approach for the coupling network is needed. To overcome this, a planar structure based on the

TABLE I
CALCULATED VALUES FOR THE EXTERNAL COUPLING AND MATCHING NETWORK USING THE DESIGN PROCESS OF [2]

| | |
|---|---|
| $C_1$ | 1.75 pF |
| $L_2$ | 0.09 nH |
| $G_L$ | 17.5 mS |

TABLE II
MAIN PARAMETERS OF THE COUPLING NETWORK

| | |
|---|---|
| $l_C$ | 1.74 mm |
| $l_L$ | 1.5 mm |
| $w_L$ | 0.22 mm |
| $l_{l4}$ | 2.48 mm |
| $w_{l4}$ | 0.19 mm |

circuit in Fig. 2 is considered. The proposed planar realization of the coupling and matching network is given in Fig. 7. The left side of (A) is directly connected to the antenna

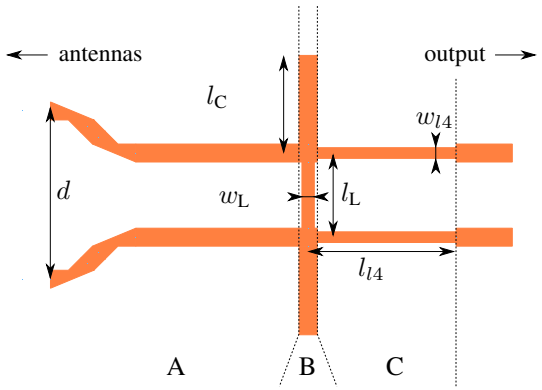


Fig. 7. Proposed coupling network scheme.

elements. (A) also brings the two feeding lines together to realize the inductor $L_2$ as a short, thin microstrip line with length $l_L$ and width $w_L$. The capacitors $C_1$ are realized by two open stubs with a length of $l_C$ each. These two elements are part of the external coupling network (B). To match the real admittance $G_L$ calculated in the design process to $50\,\Omega$, a quarter wavelength transformer with line length $l_{l4}$ and line width $w_{l4}$ is applied (C). The dimensions used in the final design at 20 GHz are given in Tab. II. All unmarked lines are $0.32\,\text{mm}$ wide, giving a characteristic impedance of $50\,\Omega$.

## IV. MEASUREMENT RESULTS

A prototype of the antenna array with and without external coupling network has been fabricated. Figure 8 shows a photograph of the backside of the prototype where the antenna feeding as well as the coupling and matching network is depicted. The total dimensions of the presented BMAA are 25 mm in length and 15 mm in width. The antenna was connected to a VNA by using a probe station for the reflection coefficient measurements and by SMP connectors for the far field measurements.

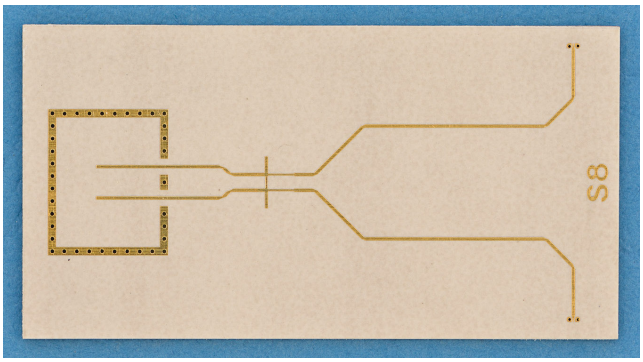


Fig. 8. Photograph of the backside of the fabricated antenna. The feeding of the patches can be seen on the left side inside the via cage. The coupling network is located in the center.

### A. Reflection coefficient

At first the reflection coefficient of the BMAA was measured. The BMAA was hereby connected using a probe station. The measurement setup was calibrated using a TRL calibration kit with the reference plane right after the coupling network. Figure 9 shows a comparison of the measured and simulated values of $|S_{11}|$. The respective simulations were carried out

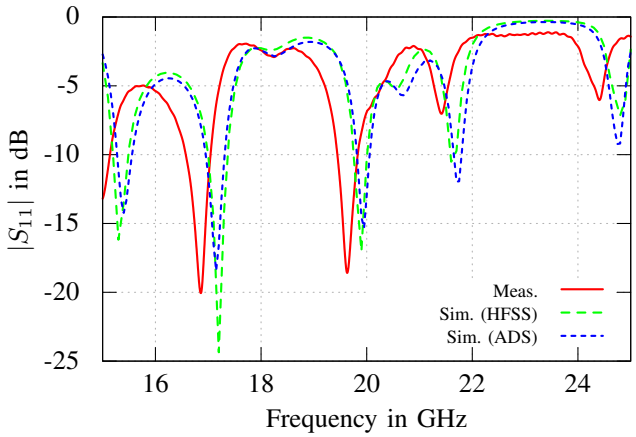


Fig. 9. Measured and simulated reflection coefficient of the BMAA.

using a full-wave 3D model [7] and a circuit model based on the system model of Section II. Both simulations showed equal results. The measurement shows a similar behaviour but is shifted by 0.4 GHz to lower frequencies. Simulations after the measurements showed that a change in the substrate permittivity to $\varepsilon_r = 3.1$ instead of the supposed $\varepsilon_r = 3$ will lead to such a frequency shift. Hence it is assumed that the actual substrate parameters differ slightly from the specified values.

The reflection coefficient curve shows some strong resonances and thereby limits the range where the BMAA can be used with good matching. The 10 dB return loss bandwidth at 19.6 GHz is around 400 MHz.

### B. Phase Gain and Output Level

The next step was the measurement of the far field properties of the BMAA. Therefore, the antenna was placed on the turntable in an anechoic chamber. A 4-Port VNA was used to connect both antenna ports as well as a measurement antenna. To compensate for the different line lengths at the antenna connections, a 3S-calibration was performed for each port to determine the error terms of the respective connections [8]. The complex radiation pattern in the H-Plane of each antenna element was measured and the relative phase $\phi_{\text{out}}$ between the antenna elements was calculated afterwards.

The fabricated BMAA showed a frequency shift when comparing the phase gain with the circuit system model. The maximum measured phase gain was obtained at 21.5 GHz. This shift in frequency compared to the results of the circuit system model could be confirmed by simulating the whole structure in a full wave simulator after the measurements.

Figure 10a shows the simulated and measured output phase difference $\phi_{\text{out}}$ at 21 GHz, Fig. 10b at 21.5 GHz. Both simulations were carried out with a modified $\varepsilon_r$ of 3.1. The full wave simulations and the measurements show an excellent match. An increase in phase progression compared to the theoretical value ($\phi_{\text{in}}$) is clearly visible in either figure. The realized phase gains, calculated according to (1), are 2.6 and 5 at 21 GHz and 21.5 GHz, respectively. The measurement at 21.5 GHz resembles the system model simulation at 20 GHz (using ADS [9]) but has a slightly lower slope in boresight direction giving a phase gain of 5 instead of 8, as designed.

To compute the output power level of the BMAA, the antenna array with strong mutual coupling without coupling network had to be measured as a reference. The power level $L_{\text{out}}$ was then calculated using (2). Figures 11a and 11b show the output power level $L_{\text{out}}$ at 21 GHz and 21.5 GHz, respectively. The power level at boresight is $-5$ dB at 21 GHz and $-7$ dB at 21.5 GHz. This corresponds to the parameters given in the design process of the BMAA.

The system model shown in Section II, however, cannot predict the exact behaviour of the output phase differences and power levels over frequency. One reason may be found in the possible inaccuracy of the Y-Parameters for higher incidence angles of the plane wave. Also the patch antennas used in this work offer some directivity compared to the monopole antennas used in [2]. This can give unwanted influences over the angle $\theta$ which are currently not covered by the system model.

## V. Conclusion

In this paper, the first design of a BMAA in the 20 GHz range was presented. All elements were realized as planar components on standard PCB technology. At 21.5 GHz, a phase gain of 5 was realized at an output level of $-7$ dB. Although the system model was found to need more improvements to predict the behaviour of the BMAA at these frequencies correctly, it was successfully proven that the concept also works in the upper microwave range, enabling

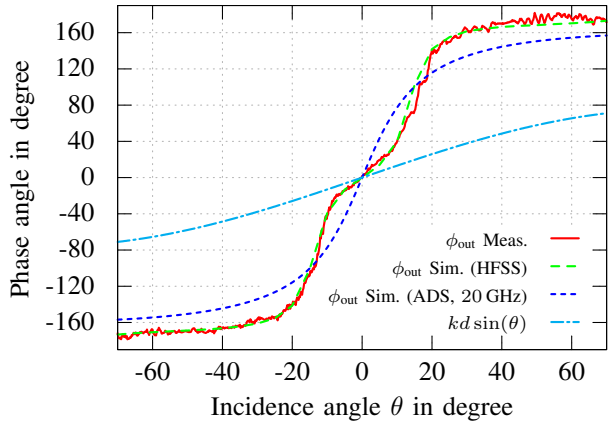


(a) 21.0 GHz

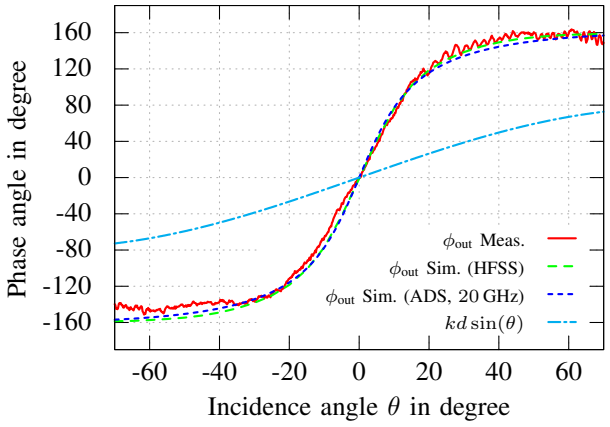


(b) 21.5 GHz

Fig. 10. Simulated and measured Phase differences at the output of the BMAA at 21.0 GHz (a) and 21.5 GHz (b). For comparison the phase difference simulated with the system model in ADS at 20 GHz is given.

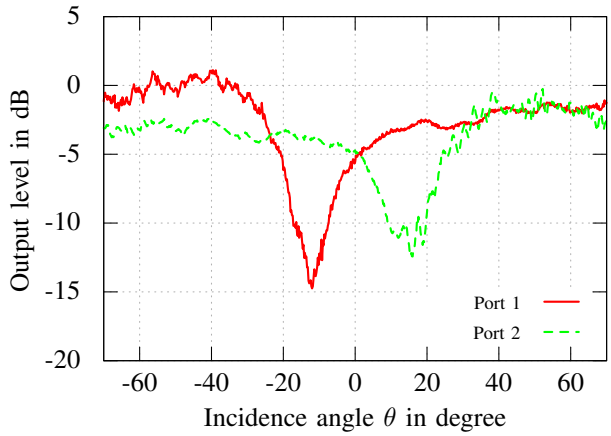


(a) 21.0 GHz

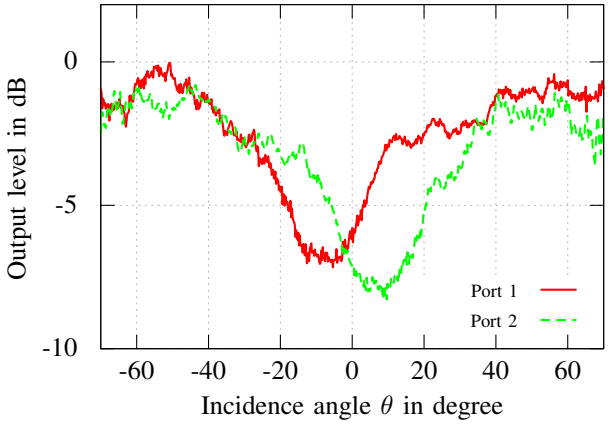


(b) 21.5 GHz

Fig. 11. Measured output power level $L_{out}$ of the BMAA at 21.0 GHz (a) and 21.5 GHz (b).

the use also in the millimeter-wave range. Using full-wave simulations instead of the circuit model, an excellent match between simulations and measurements could be obtained.

## REFERENCES


[1] R. N. Miles, D. Robert, and R. R. Hoy, "Mechanically coupled ears for directional hearing in the parasitoid fly Ormia ochracea," *The Journal of the Acoustical Society of America*, vol. 98, no. 6, pp. 3059–3070, Dec. 1995.

[2] A. Masoumi and N. Behdad, "An Improved Architecture for Two-Element Biomimetic Antenna Arrays," *IEEE Transactions on Antennas and Propagation*, vol. 61, no. 12, pp. 6224–6228, Dec. 2013.

[3] M. Akcakaya, C. Muravchik, and A. Nehorai, "Biologically inspired coupled antenna array for direction of arrival estimation," in *Conference Record of the Forty Fourth Asilomar Conference on Signals, Systems and Computers (ASILOMAR)*, Nov. 2010, pp. 1961–1965.

[4] G. Fontgalland, Z. Wang, and J. Volakis, "Small biomimetic array for direction finding and superdirectivity," in *Proceedings of URSI International Symposium on Electromagnetic Theory (EMTS)*, 2013, pp. 88–89.

[5] A. Masoumi, K. Ghaemi, and N. Behdad, "A Two-Element Biomimetic Antenna Array With Enhanced Angular Resolution and Optimized Power Extraction," *IEEE Transactions on Antennas and Propagation*, vol. 63, no. 3, pp. 1059–1066, Mar. 2015.

[6] A. Masoumi, Y. Yusuf, and N. Behdad, "Biomimetic Antenna Arrays Based on the Directional Hearing Mechanism of the Parasitoid Fly Ormia Ochracea," *IEEE Transactions on Antennas and Propagation*, vol. 61, no. 5, pp. 2500–2510, May 2013.

[7] *HFSS version 15.0.7*, ANSYS Inc., Canonsburg, PA, USA, 2014.

[8] M. Hitzler, S. Bader, and C. Waldschmidt, "Key aspects of robot based antenna measurements at millimeter wave frequencies," in *8th European Conference on Antennas and Propagation (EuCAP)*, Apr. 2014, pp. 392–396.

[9] *Agilent Advanced Design System 2014.01*, Agilent Technologies Inc., Santa Clara, USA, 2014.